J|A|C|S
ARTICLES
Published on Web 04/20/2007

Field Induced Formation of Mesoscopic Polymer Chains from Functional Ferromagnetic Colloids

Jason J. Benkoski,[†] Steven E. Bowles,[‡] Bryan D. Korth,[‡] Ronald L. Jones,[†] Jack F. Douglas,[†] Alamgir Karim,[†] and Jeffrey Pyun*,[‡]

Contribution from the Polymers Division, National Institute of Standards and Technology, Gaithersburg, Maryland 20899, and Department of Chemistry, University of Arizona, Tucson, Arizona 85721

Received February 2, 2007; E-mail: jpyun@email.arizona.edu

Abstract: The assembly and direct imaging of ferromagnetic nanoparticles into one-dimensional mesostructures (1-D) are reported. Polymer-coated ferromagnetic colloids (19 nm, 24 nm) were assembled at a crosslinkable oil−water interface under both magnetic field induced and zero-field conditions and permanently fixed into 1-D mesoscopic polymer chains (1−9 μm) in a process referred to as Fossilized Liquid Assembly (FLA). In the FLA process, nanoparticle chains were fixed at the oil interface through photopolymerization, enabling direct visualization of organized mesostructures using atomic force microscopy. Using the FLA methodology, we systematically investigated different conditions and demonstrated that *dispersed* ferromagnetic colloids possess sufficient dipolar interactions to organize into mesoscopic assemblies. Application of an external magnetic field during assembly enabled the formation of micron-sized chains which were aligned in the direction of the applied field. This universal methodology is an attractive alternative technique to cryogenic transmission electron microscopy (cryo-TEM) for the visualization of nanoparticle assembly in dispersed organic media.

Introduction

Nanoparticle assembly has been widely investigated as an approach to hierarchically ordered materials. A number of methodologies have been developed to organize nanoparticles using templates and self-assembly approaches.[1−5] In these systems, noncovalent interactions such as van der Waals or electrostatic interactions[6−8] have been widely utilized to achieve interparticle assembly. Magnetic assembly has been a subject of particular interest due to the selective directionality that is embedded in nanoparticles through dipolar associations. This directionality has been exploited to assemble iron oxide-loaded latex colloids[9−12] and emulsion droplets[9,13,14] (100 nm to 30 μm) into one-dimensional (1-D) ordered composite materials. Despite the amount of activity with larger colloids, the use of magnetic dipolar associations to organize individual nanoparticles (1 to 100 nm) remains largely unexplored. Magnetic assembly can be achieved by self-assembly or field induced processes of ferromagnetic nanoparticles into two-dimensional arrays using a "bottom up" methodology.[15] The use of magnetic nanoparticles is particularly intriguing, as organic polymers can be hybridized with inorganic colloids to form novel nanocomposite materials with synergistic properties.

Magnetic particle assembly has long been known in the fields of magnetorheological fluids and ferrofluids to enable the stimuli-responsive nature of fluid dispersions.[16,17] More recently, a number of reports have demonstrated the synthesis of uniform ferromagnetic colloids (e.g., Co, Fe) and 1-D assembly into nanoparticle chains when cast on surfaces.[18−20] Dilute solution scattering has been used to study dipolar fluids, but these techniques cannot readily differentiate between branched and

[†] National Institute of Standards and Technology.
[‡] University of Arizona.

(1) Lee, S.-W.; Mao, C.; Flynn, C. E.; Belcher, A. M. *Science* **2002**, *296* (5569), 892−895.
(2) Misner, M. J.; Skaff, H.; Emrick, T.; Russell, T. P. *Adv. Mater.* **2003**, *15* (3), 221−224.
(3) Mao, C.; Solis, D. J.; Reiss, B. D.; Kottmann, S. T.; Sweeney, R. Y.; Hayhurst, A.; Georgiou, G.; Iverson, B.; Belcher, A. M. *Science* **2004**, *303* (5655), 213−217.
(4) Lin, Y.; Boeker, A.; He, J.; Sill, K.; Xiang, H.; Abetz, C.; Li, X.; Wang, J.; Emrick, T.; Long, S.; Wang, Q.; Balazs, A.; Russell, T. P. *Nature* **2005**, *434* (7029), 55−59.
(5) Bockstaller, M. R.; Mickiewicz, R. A.; Thomas, E. L. *Adv. Mater.* **2005**, *17* (11), 1331−1349.
(6) Storhoff, J. J.; Mirkin, C. A. *Chem. Rev.* **1999**, *99* (7), 1849−1862.
(7) Shenhar, R.; Rotello, V. M. *Acc. Chem. Res.* **2003**, *36* (7), 549−561.
(8) Shenhar, R.; Norsten, T. B.; Rotello, V. M. *Adv. Mater.* **2005**, *17* (6), 657−669.
(9) Furst, E. M.; Suzuki, C.; Fermigier, M.; Gast, A. P. *Langmuir* **1998**, *14* (26), 7334−7336.
(10) Furst, E. M.; Gast, A. P. *Phys. Rev. Lett.* **1999**, *82* (20), 4130−4133.
(11) Singh, H.; Laibinis, P. E.; Hatton, T. A. *Nano Lett.* **2005**, *5*, 2149−2154.
(12) Singh, H.; Laibinis, P. E.; Hatton, T. A. *Langmuir* **2005**, *21*, 11500−11509.
(13) Goubault, C.; Leal-Calderon, F.; Viovy, J.-L.; Bibette, J. *Langmuir* **2005**, *21* (9), 3725−3729.
(14) Cohen-Tannoudji, L.; Bertrand, E.; Bressy, L.; Goubault, C.; Baudry, J.; Klein, J.; Joanny, J.-F.; Bibette, J. *Phys. Rev. Lett.* **2005**, *94* (3), 038301/1-038301/4.
(15) Sun, S. H.; Murray, C. B.; Weller, D.; Folks, L.; Moser, A. *Science* **2000**, *287*, 1989−1992.
(16) Klingenberg, D. J. *AIChE Journal* **2001**, *47* (2), 246−249.
(17) Zahn, M. *J. Nanoparticle Res.* **2001**, *3* (1), 73−78.
(18) Puntes, V. F.; Krishnan, K. M.; Alivisatos, A. P. *Science* **2001**, *291* (5511), 2115−2117.
(19) Tripp, S. L.; Puzstay, S. V.; Ribbe, A. E.; Wei, A. *J. Am. Chem. Soc.* **2002**, *124*, 7914−7915.
(20) Lalatonne, Y.; Richardi, J.; Pileni, M. P. *Nat. Mater.* **2004**, *3* (2), 121−125.

linear polymeric structures. These earlier reports were also limited by the use of magnetic nanoparticles with broad particle size distributions.[21−24]

The direct imaging of organized mesostructures in solution is a central challenge for a fundamental understanding of magnetic assembly. Analytical methods to visualize nanoparticle assembly in solution are still at an early stage of development. Recently, Klokkenburg et al. used cryogenic transmission electron microscopy (cryo-TEM) to image the zero-field self-assembly of 21 nm ferrimagnetic magnetite (Fe_3O_4) nanoparticles into flux-closure bracelets and short 1-D chains in decalin.[25] Similar reports by the same authors also visualized superparamagnetic nanoparticle assemblies of polyisobutylene coated iron colloids.[26] While cryo-TEM is a powerful technique to image dispersed colloids, difficulties in working in certain organic media can limit exploration of experimental conditions that can affect nanoparticle assembly, such as temperature, particle concentration, and applied fields.[27,28] Thus, in depth investigation of magnetic nanoparticle assembly requires measurement methods which utilize versatile sample preparation procedures coupled with imaging techniques.

Immiscible liquid interfaces have been shown to be a versatile platform for organizing polymers and nanoparticles into complex assemblies.[29−34] We have recently demonstrated that a wide range of nanoparticles can be organized at oil/water interfaces, where the oil phase can be flash-cured when exposed to UV light.[35] Nanoparticle assemblies formed at the interface are immobilized by curing of the oil phase which can then be imaged using atomic force microscopy (AFM).

Herein, we report the direct visualization of dispersed ferromagnetic nanoparticles and their mesoscale assemblies using the above described crosslinkable liquid−liquid interfacial system. Ferromagnetic colloids and nanoparticle chains formed from dipolar associations are reminiscent of nanoscale polymeric macromolecules, as ferromagnetic nanoparticle "monomers" connect via 1-D noncovalent associations to form mesoscopic polymer chains or "meso-polymers." These magnetically assembled nanoparticle chains are mesoscale analogues to other supramolecular polymers that are formed via noncovalent interactions (e.g., hydrogen bonding, metal−ligand complexation) of small molecule monomers.[36,37]

Results

Model nanoparticle materials for this study were prepared using a synthetic route we have recently developed to synthesize polystyrene coated cobalt nanoparticles (PS-CoNPs).[38] In this method, amine or phosphine oxide end-functional PS oligomers (M_n = 5000 g/mol; M_w/M_n = 1.10) were synthesized using the nitroxide mediated polymerization[39] with functional Hawker-type alkoxyamine initiators. These PS surfactants were then employed in the thermolysis of dicobaltoctacarbonyl ($Co_2(CO)_8$) in refluxing 1,2-dichlorobenzene (DCB)[18] to prepare PS-CoNPs. Coordination with ligating amine or phosphine oxide chain ends ensured stabilization of the colloidal surfaces. The encapsulating polymer shell further enabled dispersion of the cobalt nanoparticles in organic solvents, such as toluene, tetrahydrofuran (THF), and dichloromethane (CH_2Cl_2).

TEM of nanoparticles revealed that micron-sized 1-D assemblies were formed when cast onto carbon coated copper grids (Figure 1), where chains were composed of uniform cobalt colloids (Co diameter = 15 nm ± 1.5 nm, PS shell = 2 nm). X-ray powder diffraction of polymer coated nanoparticles indicated the formation of face centered cubic (fcc) metallic cobalt. Vibrating sample magnometry (VSM) confirmed that nanoparticles were weakly ferromagnetic at room temperature (saturation magnetization (M_s) = 38 emu/g, coercivity (H_c) = 100 Oe, 22 °C). Larger PS-CoNPs were also synthesized using this methodology (Co diameter = 20 nm ± 2.5 nm; PS shell = 2 nm) possessing an fcc cobalt phase and slightly enhanced magnetic properties (M_s = 38 emu/g; H_c = 254 Oe, 22 °C).

Nanoparticle assembly was performed according to the previously established method of Fossilized Liquid Assembly (FLA).[35,40] To prepare samples for imaging, PS-CoNPs were dissolved into a hydrophobic dimethacrylate monomer (1,12-dodecanedioldimethacrylate, DDMA) at different particle concentrations ((0.02%, 0.07%, 0.11%, 0.20% with a standard uncertainty of 0.005%) all percentages refer to mass fraction throughout this paper) and partitioned over a buffered aqueous phase. Assembly times before curing of the oil phase were varied from 1 to 5 min, and flash curing of the oil phase was achieved in less than 1 s. As discussed in the previous references to FLA,[35] the 1 s cure time is sufficient for particle diffusion lengths that are on the same order as the size of the particle aggregates. However, the gradual increase in viscosity and eventual gelation of the oil phase does not impose a bias on the particle diffusion paths that would lead to distortions of the final assemblies. This method therefore provides clear insight into nanoparticle interaction and the assembly process at the 2-D interface between oil−water layers (Figure 2).

The application of a magnetic field was easily achieved by placing the sample vessel under a bar magnet that generated a weak external field (8 mT ± 0.1) to organize ferromagnetic colloids. Removal of the cured poly(1,12-dodecanedioldi-

(21) Pynn, R.; Hayter, J. B.; Charles, S. W. *Phys. Rev. Lett.* **1983**, *51*, 710.
(22) Shen, L.; Stachowiak, A.; Fateen, S.-E. K.; Laibinis, P. E.; Hatton, T. A. *Langmuir* **2001**, *17* (2), 288−299.
(23) Butter, K.; Hoell, A.; Wiedenmann, A.; Petukhov, A. V.; Vroege, G. J. *J. Appl. Crystallogr.* **2004**, *37* (6), 847−856.
(24) Moeser, G. D.; Green, W. H.; Laibinis, P. E.; Linse, P.; Hatton, T. A. *Langmuir* **2004**, *20*, 5223.
(25) Klokkenburg, M.; Vonk, C.; Claesson, E. M.; Meeldijk, J. D.; Erne, B. H.; Philipse, A. P. *J. Am. Chem. Soc.* **2004**, *126* (51), 16706−16707.
(26) Butter, K.; Bomans, P. H. H.; Frederik, P. M.; Vroege, G. J.; Philipse, A. P. *Nat. Mater.* **2003**, *2* (2), 88−91.
(27) Danino, D.; Gupta, R.; Satyavolu, J.; Talmon, Y. *J. Colloid Interface Sci.* **2002**, *249* (1), 180−186.
(28) Balmes, O.; Malm, J.-O.; Karlsson, G.; Bovin, J.-O. *J. Nanoparticle Res.* **2004**, *6* (6), 569−576.
(29) Dinsmore, A. D.; Hsu, M. F.; Nikolaides, M. G.; Marquez, M.; Bausch, A. R.; Weitz, D. A. *Science* **2002**, *298*, 1006.
(30) Wong, S. M.; Cha, J. N.; Choi, K. S.; Deming, T. J.; Stucky, G. D. *Nano Lett.* **2002**, *2*, 583−587.
(31) Breitenkamp, K.; Emrick, T. *J. Am. Chem. Soc.* **2003**, *125* (40), 12070−12071.
(32) Lin, Y.; Skaff, H.; Emrick, T.; Dinsmore, A. D.; Russell, T. P. *Science* **2003**, *299* (5604), 226−229.
(33) Duan, H.; Wang, D.; Sobal, N. S.; Giersig, M.; Kurth, D. G.; Moehwald, H. *Nano Lett.* **2005**, *5* (5), 949−952.
(34) Duan, H.; Kuang, M.; Wang, D.; Kurth, D. G.; Moehwald, H. *Angew. Chem., Int. Ed.* **2005**, *44* (11), 1717−1720.
(35) Benkoski, J. J.; Hu, H.; Karim, A. *Macromol. Rapid Commun.* **2006**, *27*, 1212.
(36) Brunsveld, L.; Folmer, B. J. B.; Meijer, E. W.; Sijbesma, R. P. *Chem. Rev.* **2001**, *101* (12), 4071−4097.
(37) Hoeben, F. J. M.; Jonkheijm, P.; Meijer, E. W.; Schenning, A. P. H. J. *Chem. Rev.* **2005**, *105* (4), 1491−1546.
(38) Korth, B. D.; Keng, P.; Shim, I.; Bowles, S. E.; Tang, C.; Kowalewski, T.; Nebesny, K. W.; Pyun, J. *J. Am. Chem. Soc.* **2006**, *128*, 6562−6563.
(39) Hawker, C. J.; Bosman, A. W.; Harth, E. *Chem. Rev.* **2001**, *101* (12), 3661−3688.
(40) Benkoski, J. J.; Jones, R. L.; Douglas, J. F.; Karim, A. *Langmuir* **2007**, *23*, 3530−3537.

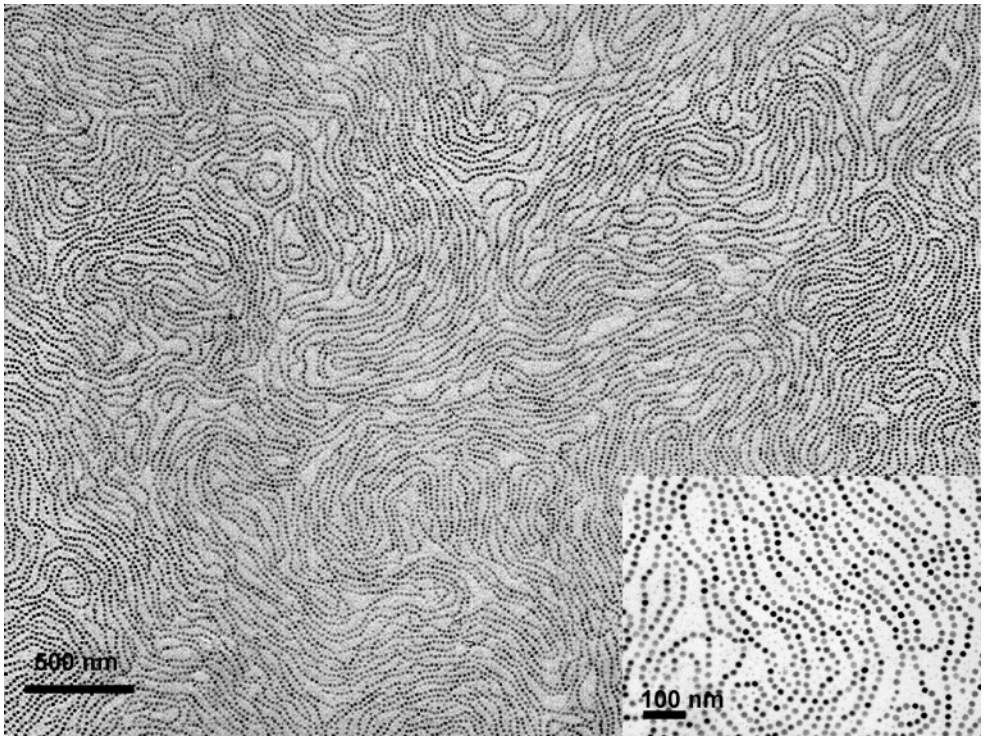

Figure 1. TEM of ferromagnetic PS−Co nanoparticles (diameter = 19 nm) drop cast in zero field onto carbon coated TEM grids from CH_2Cl_2/DCB (10:1 ratio by volume). 1-D assemblies of meso-polymer chains on a surface formed from dipolar associations between ferromagnetic colloids.

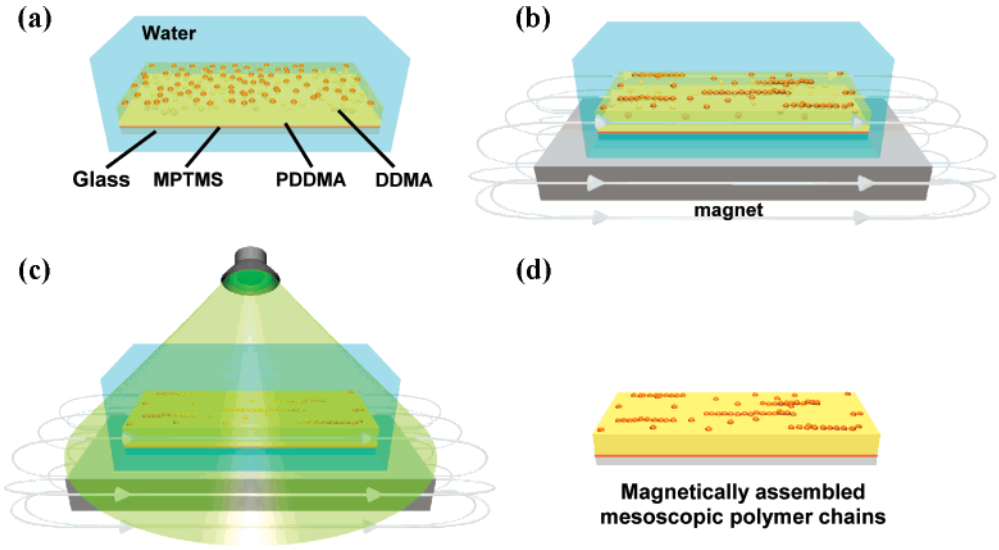

Figure 2. Schematic of Fossilized Liquid Assembly (FLA). The PS−Co nanoparticles are initially dispersed in the DDMA, sonicated, and then placed on a glass slide that is precoated with a layer of silane adhesion promoter and a layer of crosslinked DDMA (PDDMA). (a) Next, the oil-coated glass slide is immersed in water. (b) A permanent magnet is placed below the sample, giving an applied field of 8 mT. (c) Once the particles are given time to segregate to the interface and align with the magnetic field, the sample is "fossilized" by crosslinking the DDMA with UV light. (d) Finally, the sample is rinsed with deionized water and dried with nitrogen prior to inspection.

methacrylate) (PDDMA) crosslinked phase from water enabled *ex situ* imaging of nanoparticle assemblies using AFM on the interface. Using this system, visualization of nanoparticle assemblies formed under varying conditions of particle concentration, applied field strength, and assembly time was achieved.

To determine whether dispersed ferromagnetic nanoparticles were capable of forming dipolar associations, 19 nm PS−Co colloids samples were assembled at 22 °C (±1 °C) for 5 min in zero field and under an 8 mT magnetic field (Figure 3a). For samples prepared in zero field, AFM images revealed the presence of short nanoparticle chains that at this length scale resembled a self-avoiding random walk in 2-D. These mesostructures ranged from several hundred nanometers to microns in length, and 19 nm in width. Irregularly branched mesostructures and flux-closure rings were also observed in zero-field, self-assembled conditions. It is important to note that the morphologies of ferromagnetic PS−Co colloids assembled in zero-field and applied field conditions strongly correlate with the Monte Carlo simulations of Chantrell et al. for similar 15 nm dipolar Co nanoparticles.[41,42] Douglas and co-workers also observed the formation of similar polymeric structures using

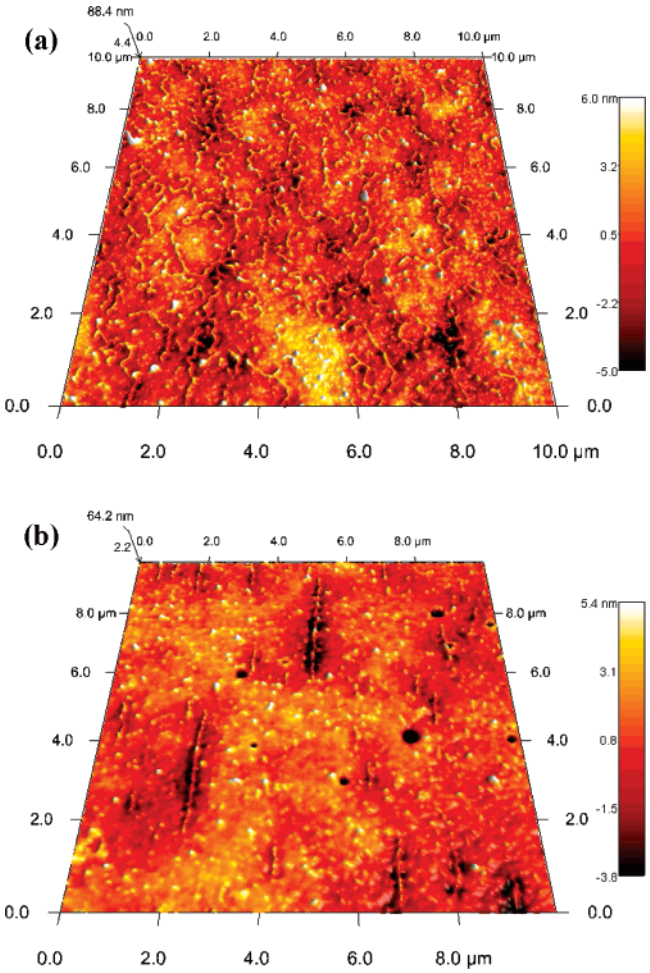

Figure 3. PS−Co nanoparticles (19 nm) assembled and embedded in PDDMA matrices after assembly and UV curing for 0.11% particle loading, temperature = 22 °C, assembly time = 5 min for (a) zero-field, self-assembled conditions and (b) 8 mT applied magnetic field at a concentration of 0.20%. Note that linear and branched nanoparticle assemblies are formed in zero field, while only rigidified nanoparticle chains are present in magnetically assembled structures.

3-D and 2-D Monte Carlo simulations and for experiments interrogating near two-dimensional granular magnetic particle fluids.[43,44]

A strikingly different morphology was observed for identical PS−CoNP samples developed under an applied magnetic field (Figure 3b). AFM revealed the formation of rigid, 1-D nanoparticle chains spanning microns in length composed of single colloidal repeating units aligned in the direction of the applied external field. These structures closely correlate with Monte Carlo simulations performed by Stevens and Grest examining the case of soft sphere dipoles and Stockmayer fluids in an external magnetic field.[45−47] Chain lengths of assembled mesosopic polymer chains were not uniform, but all nanoparticle assemblies were imaged as discrete individual mesostructures that did not form laterally bundled aggregates.

To probe the effect of particle concentration on the assembly process, 19 nm PS−CoNP samples were prepared at different loadings (0.01%, 0.07%, 0.11%, 0.20%), with other sample variables held constant (22 °C for 5 min, 8 mT applied field). AFM imaging of these various samples indicated that aligned meso-polymer chains were formed. However, the assembled structures prepared at higher concentration displayed a trend toward longer chain lengths (Figure 4). Beyond a concentration of about 0.20%, the interface was almost fully covered with particles, meaning that particle aggregates were difficult to distinguish from the free particles. Small aggregates of ferromagnetic nanoparticles (e.g., dimers, trimers) are also imaged at high particle concentrations as sharp bright globular protusions, which reside slightly above meso-polymer chains in the oil−water interfacial plane. The observed dependence of chain length on concentration resembles the mechanism of supramolecular polymerizations and self-assembled supramolecular 1-D fibers that exhibit a strong dependence of the morphology of organized structures on monomer precursor concentration.[36,48]

Furthermore, when larger 24 nm Co nanoparticles (M_s = 38 emu/g; H_c = 254 Oe) were assembled at oil−water interfaces, the formation of rigid 1-D mesostructures was observed spanning length scales up to 9 μm. Meso-polymers of this length are composed of approximately 370 PS−Co nanoparticle repeat units (Figure 5). Lateral bundling of assembled meso-polymer chains was not observed under the conditions of FLA imaging. This is likely due to the low concentration of PS-CoNPs used in these experiments. However, the time utilized to prepare samples for FLA is likely much faster than the time scale required for lateral association of assembled meso-polymer chains. Additionally, sedimentation of meso-polymers of sufficient size and density can occur out of the plane of the oil−water interface. Evidence of this sedimentation is captured in Figure 5, as a slight collapse of the crosslinked DDMA phase around the micron sized meso-polymer chain is imaged using AFM. Future microtoming and TEM studies of PS-CoNPs and meso-polymer chains embedded in the crosslinked DDMA phase are in progress to confirm whether significant sedimentation away from the oil−water interface occurs.

To evaluate the reversibility of the assembly process, PS−CoNP assemblies were formed in an 8 mT field for 2.5 min and allowed to equilibrate in the absence of an external field for an additional 2.5 min before UV curing (Figure 6). AFM visualization indicated that the conformation of the nanoparticle assemblies was consistent with irregular branched and bracelet mesostructures formed solely under zero-field conditions. These results suggest that while this system may not be completely reversible under these conditions, the meso-polymer chains are able to relax into nearly random conformations due to thermal fluctuations. The presence of shorter chains was attributed to either nucleation events after removal of the applied field or fragmentation of larger mesostructures.

Discussion

The appearance of the meso-polymers after the removal of the external field warrants discussion of magnetic assembly

(41) Chantrell, R. W.; Bradbury, A.; Popplewell, J.; Charles, S. W. *J. Phys. D: Appl. Phys.* **1980**, *13* (7), L119−L122.
(42) Chantrell, R. W.; Bradbury, A.; Popplewell, J.; Charles, S. W. *J. Appl. Phys.* **1982**, *53* (3, Pt. 2), 2742−2744.
(43) Stambaugh, J.; van Workum, K.; Douglas, J. F.; Losert, W. *Phys. Rev. E* **2005**, *72*, 031303.
(44) van Workum, K.; Douglas, J. F. *Phys. Rev. E* **2005**, *71*, 031502.
(45) Stevens, M. J.; Grest, G. S. *Phys. Rev. Lett.* **1994**, *72* (23), 3686−9.
(46) Stevens, M. J.; Grest, G. S. *Phys. Rev. E* **1995**, *51* (6-A), 5976−83.
(47) Stevens, M. J.; Grest, G. S. *Phys. Rev. E* **1995**, *51* (6-A), 5962−75.
(48) Jonkheijm, P.; Hoeben, F. J. M.; Kleppinger, R.; Van Herrikhuyzen, J.; Schenning, A. P. H. J.; Meijer, E. W. *J. Am. Chem. Soc.* **2003**, *125* (51), 15941−15949.

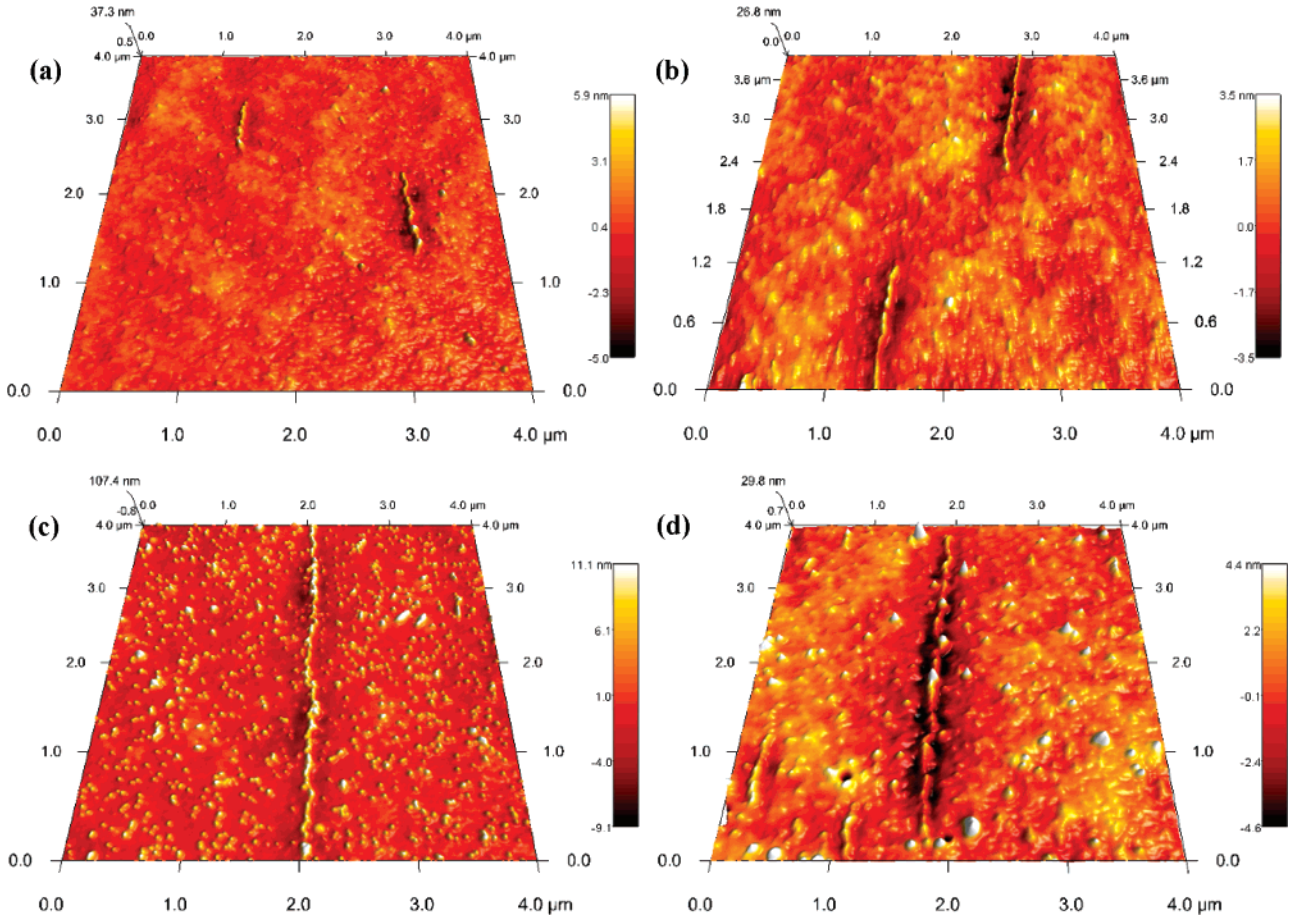

Figure 4. AFM height image of 19 nm PS−Co nanoparticle chains assembled under the influence of an 8 mT magnetic field. The concentrations are as follows: (a) 0.01%, (b) 0.07%, (c) 0.11%, (d) 0.20%; assembly time was 5 min for all samples.

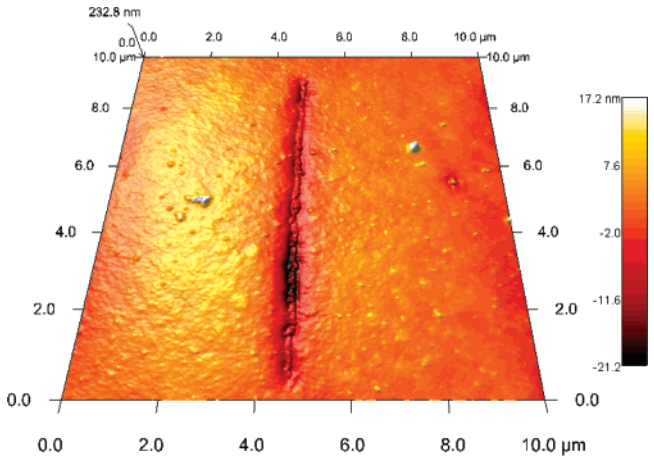

Figure 5. AFM height image of an aligned meso-polymer chain assembled under the influence of an 8 mT magnetic field from 24 nm PS−Co nanoparticles.

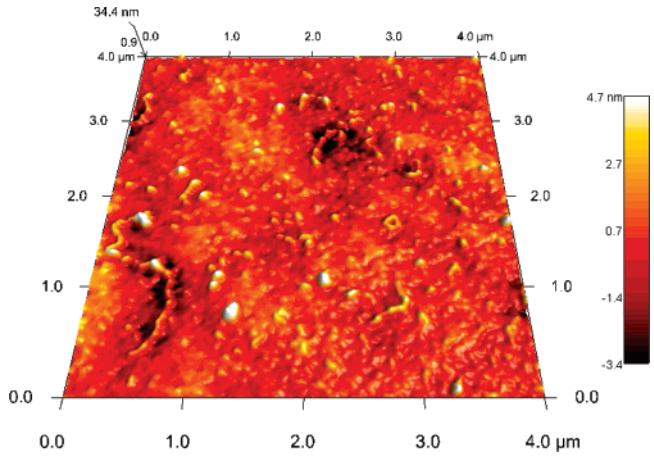

Figure 6. AFM height images obtained at a concentration of 0.07% PS−Co nanoparticles (19 nm) by mass. This sample was allowed to assemble under the influence of an 8 mT magnetic field for 2.5 min and then in zero field for an additional 2.5 min.

under the influence of an applied field. In contrast to the rigid aligned chains organized using applied fields, meso-polymers formed under zero field conditions exhibit morphologies resembling self-avoiding random walks. While different assembled morphologies were expected, certain features, namely, the higher surface coverage of meso-polymers at oil interfaces per unit area as imaged in Figure 3a in comparison to all field-induced assembled samples (Figures 3b, 4, 5), were counter-intuitive.

Naively, the effect of external fields was anticipated to generate a preferred head-to-tail alignment of the particles and form a greater number of chains per unit area. However, closer examination revealed that the uniform dipole orientation causes a second possibility—side-by-side particles with aligned dipoles resulting in dipolar repulsion. This angular dependence of the dipolar interaction effectively eliminates half of the possible particle binding events by making it impossible for particles to

bind with each other when they approach from a direction that is orthogonal to the applied field ($\pm\pi/4$ radians). In contrast, approaching particles in zero field freely rotate to align with each other and enhance the dipolar attraction when brought into contact.

An additional issue for field-induced assembly is the contribution of magnetic field gradients exerting a force on the magnetic particles that induce translation toward the increasing magnetic flux. However, the current experiments were designed to avoid such gradients in the plane of the oil/water interface. It was therefore anticipated that magnetic dipoles of the individual particles would be rotationally aligned with the external magnetic field but exhibited similar diffusion paths as those from random Brownian motion.

These two observations explain the prevalence of monomers (i.e., free nanoparticles) in imaging experiments conducted using particle concentrations as high as 0.11%. Comparison of field induced (Figure 4c) and zero-field (Figure 3a) conditions for assembly clearly illustrate the effect of external fields on the surface coverage of organized meso-polymers at the oil−water interface. Although AFM does not provide large statistics, the 20 μm and 50 μm scans of the 0.11% samples indicate that the areal density of meso-polymers under an 8 mT field was about an order of magnitude lower than for zero-field conditions. However, the average length of the meso-polymers was comparable, if not longer, when the external field was applied. Such comparisons are especially noteworthy, because the total number of particles per unit area did not appear to change, despite the dramatic difference in the areal density of meso-polymer chains.

Taken together, these details point to a polymerization mechanism whereby individual nanoparticles are rotationally aligned with the external field, but undergo random Brownian motion. Nanoparticle contacts along the N−S flux lines are attractive, while lateral interactions are repulsive. Despite the presence of a dipolar attraction, random Brownian motion of individual ferromagnetic nanoparticles is initially achieved due to the low particle concentrations used in the experiment and rigorous ultrasonic sonication of samples immediately before FLA. Particles adjacent to a growing meso-polymer will not generally be attracted to the side of the chain. Although aligned dipolar particles are attracted to each other when they stack in a staggered, zigzag pattern, the window for a successful approach is quite narrow since the dipolar interaction switches sign as soon as the particles move along the chain by a half repeat unit.

The best sites for particle addition, therefore, are the chain ends. The critical areas of interest are the regions over which the particles can diffuse within 5 min, as indicated in FLA assembly experiments. To a first approximation,[49] one can calculate the average distance, x, that a particle diffuses in time, t,

$$x = \sqrt{\frac{k_B T t}{6\pi\eta\, a}} \qquad (1)$$

where k_B is Boltzmann's constant, T is temperature, η is the viscosity, and a is the particle radius. For a measured viscosity of 15 mPa·s for DDMA, the typical diffusion distance is about 15 μm for a 19 nm particle (15 nm diameter Co nanocrystal with a 2 nm thick PS shell). Since the area itself is large, the likelihood of monomer depletion at the chain ends is fairly low.

The rate of initiation, which appears to be slower in the case of an applied field, is probably controlled by a different process. The rate-limiting step may be the amount of time it takes for stochastic processes to form a seed chain beyond a critical length. In addition, the initiation rate may be reduced by removing the orientational degree of freedom. Despite these possibilities, the equilibrium Monte Carlo simulations by Stevens and Grest did not give any indication that the areal density of meso-polymers would be suppressed by an applied field.[45−47] In fact, these authors observed the more intuitive result that meso-polymer formation was enhanced with increasing field strength. One additional possibility may account for this discrepancy. While the driving force for interfacial segregation appears to be sufficient for maintaining particle aggregates at the interface, the high density of cobalt (9 g/cm^3) means that larger aggregates will tend to sediment to the bottom of the oil phase. Supposing that applied magnetic fields do lead to longer aggregates, a significant population of nanoparticles would reside below the oil−water interface and would therefore be inaccessible to AFM. Previous studies of magnetite nanoparticle assembly using FLA showed strong evidence of such sedimentation.[40] The difference in the current system is that, if such sedimentation has occurred, the subsurface aggregates are too small to be seen by optical microscopy. To obtain a more detailed understanding of the initiation process, studies are currently underway that involve taking time slices of the assembly process, which are performed by flash curing a series of identical samples at different times. High-resolution images may also shed light on whether the spatial distribution of free particles is depleted in the vicinity of the chain ends.

Conclusions

The 1-D magnetic assembly of polymer coated ferromagnetic colloids into mesoscopic polymer chains using a novel liquid−liquid interfacial system is reported. Using a novel model colloid system, we demonstrate that dispersed ferromagnetic nanoparticles possess sufficient dipolar attractions to self-assemble or organize under an applied field into mesostructured materials. This versatile methodology enables facile evaluation of magnetic assembly conditions and demonstrates the potential of this bottom-up approach to prepare organized 1-D mesoscale materials.

Experimental Section

Materials and Instrumentation. Irgacure 819 (bis(2,4,6-trimethylbenzoyl)phenyl-phosphine oxide) was purchased from Ciba Specialty Chemicals and used as received. 1,12-Dodecanediol dimethacrylate (DDMA) and *N*-(2-hydroxyethyl)piperazine-*N*′-2-ethanesulfonic acid (HEPES) were purchased from Aldrich and used as received.[35] Tapping mode atomic force microscopy was conducted using an Asylum Research MFP-3D AFM scope. TEM images were obtained on a JEM100CX II transmission electron microscope (JEOL) at an operating voltage of 60 kV, using in-house prepared copper grids (Cu, hexagon, 270 mesh).

Synthesis of Polystyrene Coated Ferromagnetic Colloids. Cobalt nanoparticles were synthesized using amine and phosphine oxide terminated polystyrene (PS) surfactants in the thermolysis of dicobaltoctacarbonyl ($Co_2(CO)_8$) in refluxing 1,2-dichlorobenzene (DCB)

(49) Einstein, A. *Investigations of the Theory of Brownian Movement*; Dover: New York, 1956.

yielding uniform ferromagnetic colloids (particle size Co core = 15 nm ± 1.5 nm; PS shell = 2 nm; M_s = 38 emu/g, H_c = 100 Oe at room temperature). Larger PS-coated cobalt nanoparticles were prepared using a similar methodology except using a two-stage temperature ramp (180 °C-particle nucleation; 150 °C-particle growth) in the thermolysis of $Co_2(CO)_8$ (particle size = 20 nm ± 2.5 nm; PS shell = 2 nm; M_s = 38 emu/g; H_c = 254 Oe at room temperature).[38]

Sample Preparation for Fossilized Liquid Assembly.[35,40] PS−Co colloids were first dispersed in bulk DDMA by sonication for 30 min. The system consists of an oil phase, a water phase, and a solid glass support for the oil phase. To promote wetting and adhesion with the oil phase, the glass slide was pretreated with (3-trimethoxylsilyl)propyl methacrylate and crosslinked DDMA.

The oil phase consisted of DDMA modified with 2% Irgacure 819 by mass fraction (all percentages refer to mass fraction throughout this paper) to promote rapid crosslinking during UV light exposure. With a viscosity of 15 mPa·s, DDMA has similar flow properties to water at room temperature (0.89 mPa·s). The interfacial tension between these two fluids is approximately 15 mJ/m^2 at 25 °C, which is of the same order as that between water and cooking oil. When exposed to a 365 nm high-pressure mercury lamp at an intensity of 8 mW/cm^2, the oil phase solidifies in less than 1 s. The aqueous phase was buffered using 10 mmol/L HEPES. The pH was adjusted to 8, and the salt concentration was fixed at 100 mmol/L NaCl to help prevent emulsification of water in the oil phase. Sample preparation was varied with respect to particle loading (0.01, 0.02, 0.07, 0.11, and 0.20 wt %), temperature (22 and 50 °C), assembly time before UV curing (1, 5, 15, 30, and 60 min), and the application of an external magnetic field (8 mT). Magnetic fields were applied by placing the sample vessel above an AlNiCo hand magnet.

Acknowledgment. Fellowship support from National Research Council is gratefully acknowledged. We also acknowledge the financial and technical support from the Polymers Division at NIST, the ACS-PRF, the Information Storage Industrial Consortium (INSIC), and the University of Arizona.

JA070779D